Journal of Zhejiang University-SCIENCE B (Biomedicine & Biotechnology)
ISSN 1673-1581 (Print); ISSN 1862-1783 (Online)
www.jzus.zju.edu.cn; www.springerlink.com
E-mail: jzus@zju.edu.cn

Toxicity testing of four silver nanoparticle-coated dental castings in 3-D LO2 cell cultures*

Yi-ying ZHAO[1], Qiang CHU[†‡1], Xu-er SHI[1],
Xiao-dong ZHENG[1], Xiao-ting SHEN[2], Yan-zhen ZHANG[†‡3]

[1]*Department of Food Science and Nutrition, Zhejiang Key Laboratory for Agro-Food Processing, Fuli Institute of Food Science, Hangzhou 310058, China*

[2]*Huajiachi Dental Center, Stomatology Hospital Affiliated to Zhejiang University of Medicine, Hangzhou 310006, China*

[3]*Department of General Dentistry, the Second Affiliated Hospital, School of Medicine, Zhejiang University, Hangzhou 310012, China*

[†]E-mail: 31300100694@zju.edu.cn; zyz85@hotmail.com

Received Oct. 22, 2016; Revision accepted Jan. 3, 2017; Crosschecked Jan. 8, 2018

Abstract: To address the controversial issue of the toxicity of dental alloys and silver nanoparticles in medical applications, an in vivo-like LO2 3-D model was constructed within polyvinylidene fluoride hollow fiber materials to mimic the microenvironment of liver tissue. The use of microscopy methods and the measurement of liver-specific functions optimized the model for best cell performances and also proved the superiority of the 3-D LO2 model when compared with the traditional monolayer model. Toxicity tests were conducted using the newly constructed model, finding that four dental castings coated with silver nanoparticles were toxic to human hepatocytes after cell viability assays. In general, the toxicity of both the castings and the coated silver nanoparticles aggravated as time increased, yet the nanoparticles attenuated the general toxicity by preventing metal ion release, especially at high concentrations.

Key words: LO2 cell; 3-D model; Silver nanoparticles; Dental alloys; Toxicity test
https://doi.org/10.1631/jzus.B1600482 **CLC number:** Q813.1+1

1 Introduction

Though dental alloys have been widely used in modern dentistry as casting materials, concerns over their biological safety still exist (Wataha, 2000). Various toxicity tests have been conducted to investigate the application safety of these materials with some positive reports finding them to be non-toxic (Schmalz et al., 1998) and other negative studies finding that they are toxic (Al-Hiyasat et al., 2002). At the same time, with the emergence of nanotechnologies, silver nanoparticles are now applied to dental biomaterials (Hamouda, 2012) due to their great antimicrobial effects (Morones et al., 2005) and anti-inflammatory properties (Wong et al., 2009). Yet the application of this material also remains controversial due to the possible metal toxicity (Allaker, 2010) and the specific nanotoxicity (Fadeel and Garcia-Bennett, 2010) of the particles. So far, many cytotoxicity tests of silver nanoparticles and the releasing of silver ions into human cells have shown irreversible cell death, decreased mitochondrial functions (Hussain et al., 2005; AshaRani et al., 2009), and dose-dependent sensibility (García-Contreras et al., 2011), raising the concerns to an even higher level.

Generally, the toxicity of metallic materials derives from the fluid environment in the human body

‡ Corresponding authors
* Project supported by the Zhejiang Provincial Natural Science Foundation of China (No. LZ14C200001) and the Public Welfare Project of Science Technology Department of Zhejiang Province (No. 2013c33139), China
ORCID: Yi-ying ZHAO, https://orcid.org/0000-0002-9517-9669

where metal corrosions initiate, leading to the diffusion of metal ions into the surrounding tissue (Ren et al., 2002) and may thus cause toxicity, inflammation, and allergic reaction in the recipients (Aksakal et al., 2004). To assess the toxicity of such materials, specific tests were conducted mainly on monolayer models using murine fibroblasts and osteoblastic cells (Yamamoto et al., 1998). Though improvements have been made to enable a more thorough study of metal cytotoxicity (Hanawa, 2002), the effectiveness of these cell models is still limited by cell types and the 2-D morphology.

Though fibroblasts and osteogenic cells may be suitable for electrochemical analysis (Hiromoto et al., 2002), for cell adhesion experiments (Zreiqat et al., 2002), or for testing cytotoxicity in surrounding tissues (usually bones and vessels), using only these cells is not enough for a thorough toxicity test. Increased concentrations of corroded particles have been found in tissues both near the implants and in other parts of the body such as the liver, which has been identified as the major target tissue for prolonged silver nanoparticle exposure (Sung et al., 2008). This means that cytotoxicity tests of other tissues, especially the liver, are also required when assessing the general toxicity of metallic materials due to the dissolution of metal ions and other chemicals in the circulating body fluids.

In this study, LO2 cells are selected as the cultured cell representing tissue from the biggest digestive gland (Kmieć, 2001), the liver, where 90% of medicines are metabolized by cytochrome P450 enzymes (CYP450) (Dambach et al., 2005) with most of them producing efficacy or toxicity afterwards (Gómez-Lechón et al., 2007). Besides, the liver is super sensitive to xenobiotics and is subject to damage by medicine doses several times lower than that which damages other organ tissues (Burcham, 2014). In pharmaceutics, hepatocyte models are widely used to evaluate the hepatotoxicity of a medicine and are considered relatively mature in application. Moreover, the innovative model used here addresses the limitation of traditional 2-D models to form cell organoids. These types of cell aggregates are able to maintain high-level cell performances (Niinomi et al., 2002) and therefore have been advocated to best mimic the in vivo microenvironment of liver tissues.

The objective of this study was to build up an in vivo-like 3-D model through gel entrapment culture and further, to prove the superiority of the 3-D model in toxicity testing compared with the traditional monolayer model used in the field. Later, toxicities of the sliver nanoparticle-coated dental castings were evaluated in the 3-D model to determine the safe usage of the alloys in practical application.

2 Materials and methods

2.1 Materials

Polyvinylidene fluoride (PVDF) hollow fiber materials (aperture 0.2 μm, pure water flux 800 L/(m^2·h) under 0.1 MPa, inner/outer diameter 0.7 mm/1.3 mm) were purchased from the SENUO Filtration Technology Co., Ltd. (Tianjin, China). Rat-tail collagen, 3-(4,5-dimethyl-2-thiazolyl)-2,5-diphenyl-2-H-tetrazolium bromide (MTT), and Hoechst 33258 dying were purchased from the Sigma-Aldrich (St. Louis, MO, USA). Urea, albumin, and lactate dehydrogenase (LDH) kits were purchased from the Nanjing Jiancheng Bioengineering Institute (Nanjing, China). Fetal bovine serum (FBS) and cell lysis buffer were purchased from the Beyotime Institute of Biotechnology Ltd. (Shanghai, China). $AgNO_3$ and $NaBH_4$ are of analytical grade and were purchased from the Aladdin Reagent (Shanghai, China). Wirobond C (WC), Keragen (KN), Ceramill Sintron (CS), and Solibond C plus (SCP) cobalt-chromium alloys were bought from the BEGO (Germany), the Dentalwaren ED GmbH (Germany), the Amanngirrbach (Germany), and the YETI Dentalprodukte GmbH (Germany), respectively.

2.2 Cell culture and treatments

The cell were cultured according to the methods described by Chu et al. (2017). Briefly, for the monolayer culture, LO2 cells were cultured in Dulbecoo's modified Eagle medium (DMEM, Gibco) containing 100 U/ml streptomycin, 100 U/ml penicillin, and 10% (v/v) FBS, and were later incubated at 5% (v/v) CO_2, 37 °C. For the 3-D culture, DMEM culture medium was first mixed with 2 g/L collagen at a ratio of 1:1 (v/v) for later usage. LO2 cells were calculated for the appropriate seeding density and were then mixed with the previous solution. After adequate mixing, 20 μl of the final solution was injected into the lumen of a 3-cm long sterilized PVDF hollow fiber. To stabilize the collagen, the hollow fibers were kept for 10 min at

37 °C. Later, a certain number of hollow fibers were put into the 6-well plate with 2 ml preheated culture medium and were incubated at 5% CO_2, 37 °C. After reaching the appropriate confluence, the cells were washed with phosphate buffer saline (PBS) twice and treated with extracts. Cells with no treatment (medium only) were used as the negative control.

2.3 Preparation of the dental casting samples

A waxing model sized 10 mm×10 mm×2 mm was created, and the samples were made using the lost-wax method. The surfaces of the castings were polished using abrasive paper of 100, 200, 400, and 800 meshes successively to acquire the same coarseness.

2.4 Preparation of the silver nanoparticle-coated dental castings

The spherical silver nanoparticles were prepared using hydrothermal methods according to the reaction: $AgNO_3+NaBH_4 \rightarrow Ag+1/2H_2+1/2B_2H_6+NaNO_3$.

$AgNO_3$ solutions (0.5, 1.0, and 2.5 ml) were added to $NaBH_4$ solutions to produce silver nanoparticles of low, medium, and high concentrations, respectively. After 30 min of magnetic stirring, 12 ml of each final solution, together with the sample castings, was put into the hydrothermal reactors for 2 h at 130 °C. Later, the coated alloys were cooled and dried at 80 °C.

2.5 Preparation of the dental castings extract

The castings were first marked and went through steamed sterilization. After drying, each of the 1 cm^2-sized castings was immersed into 2 ml of culture medium based on the ISO requirement (0.5 to 0.6 cm^2/ml) for 7 d before further toxicity testing. Later, the extracts went through filtration using 0.22-μm micro porous membranes.

2.6 Cell viability assays

For the monolayer culture, the cells were immersed in 0.5 mg/ml MTT for 4 h in the incubator at 5% CO_2, 37 °C. At the end of the incubation, 150 μl dimethyl sulfoxide (DMSO) was added to dissolve the formazan precipitate. For the 3-D culture, the hollow fiber reactors were immersed in 2 ml 0.5 mg/ml MTT-PBS in each well and were later incubated for 4 h. At the end of the incubation, the hollow fibers were transferred into a 2-ml centrifuge tube and were cut up into pieces. DMSO (750 μl) was added to dissolve the formazan precipitate. The absorbance was measured at 570 nm using a spectrophotometer. This method is referred to the one described by Chu et al. (2017).

2.7 Fluorescent stain of nuclei

The hollow fibers were first taken out and cut in the straight direction. The cells were scraped from the inner surface of the hollow fibers and were then immersed in 10 μg/ml Hoechst 33258 solution for 30 min of cultivation at 37 °C. Later, the dying solutions were discarded and PBS was used to rinse. The cells were observed under the phase contrast fluorescent microscope. This method is referred to the one described by Chu et al. (2017).

2.8 Statistical analysis

All experiments were carried out at least three times. The results were expressed as mean±standard deviations (SD) and analyzed by one-way analysis of variance (ANOVA) using SPSS (Version 19.0). $P<0.05$ was considered statistically significant, and graphs were drawn by GraphPad Prism 6.0 for Windows (GraphPad Software, San Diego, CA, USA).

3 Results and discussion

3.1 Characterization of the hollow fiber materials

Based on the bioreactor technology, hollow fiber polymers were used as supporting materials when forming LO2 cylindroids within the model. The material used here is known for its great performance in chemical stability, radiation resistance, heat resistance (Li and Lv, 2001), and other general properties. It is the key component of the model assuring both cell growth and material exchange between inner cells and the outside culture medium.

Scanning electron microscope (SEM) images in Fig. 1 show the inner surface of the PVDF under both cross cut and straight cut directions and different amplification factors. As seen from the pictures, the inner surface of the material was rather rough, indicating its ability to support tight cell adherence, good growth, normal proliferation, and high-level functional expression of the cells. The massive micro pores presented also demonstrated the ability of the hollow fiber to exchange materials between the inner

cells and the outer culture medium. Moreover, since these fibers went through steam sterilization to reach the high-standard disinfection of microorganisms, the small diameters and shapes of the pores also suggested a favorable heat resistance ability. All these characteristics combined confirmed the feasibility of using sterilized PVDF material to construct the bioreactor according to its high permeability and capacity for maintaining cell growths (de Bartolo et al., 2006). In this section, we conducted the same type of experiment presented by Chu et al. (2017) to assure the integrity and effectiveness of this particular batch of materials.

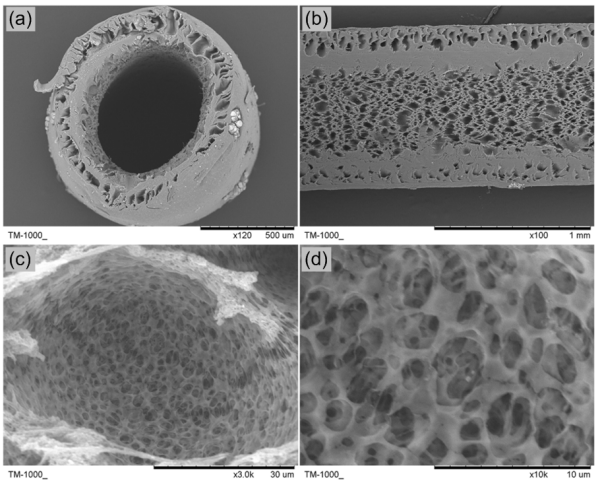

Fig. 1 SEM images of PVDF hollow fibers after sterilization
(a) Cross cut image of hollow fiber with amplification factor of 120×. (b–d) Straight cut images of hollow fiber with amplification factors of 100× (b), 3000× (c), and 10000× (d)

3.2 Characterization of the silver nanoparticle-coated alloys

SEM images were observed to ensure the successful preparation of the nanoparticles and their adhesion to the dental castings. As seen from Fig. 2, round shaped nanoparticles were scattered across the alloy surface and the overall coverage area increased along with higher nanoparticle concentrations. Later, spectrum analysis was conducted on a piece of KN alloy coated with low-concentration nanoparticles to analyze the metal compositions (Fig. 3 and Table 1) of the combined biomaterials. Within the detected area, four elements Cr, Co, Ag, and W were confirmed, weighting 26.46%, 59.35%, 0.94%, and 13.25% of the overall materials, respectively.

3.3 Construction and optimization of the model

This model used rat tail collagen type I to create the entrapment culture of LO2 cells within the hollow fiber. The collagen used here had two major functions: to ensure the formation of cell aggregates and to improve the long-term bioactivity and integrity of the cells by providing better adhesion to the scaffolds (Kino et al., 1998). Here, the hollow fibers and collagen worked as blood vessels and liver connective tissue, respectively, to mimic the microenvironment of liver tissue.

After primary construction, cell seeding density was optimized to ensure the best performance of the cells. Mixed with 2 mg/ml collagen solution, cell suspension with concentrations varying from 1×10^4 to 5×10^6 cells/ml was injected into the hollow fiber model. The number of hollow fibers placed in the 6-well plates was carefully calculated to ensure an equal cell growth area in both the 3-D and the monolayer models. After 4-d cultivation, the bioactivity of cells within the two models was determined. As seen from Fig. 4a, urea synthesis in the 3-D model was greater than the monolayer one at lower cell seeding density from 1×10^4 to 5×10^5 cells/ml. While at cell seeding density of 5×10^4 and 1×10^5 cells/ml, significant differences were observed. Albumin secretion was also measured (Fig. 4b). In general, albumin secretion in the 3-D model remained roughly the same with

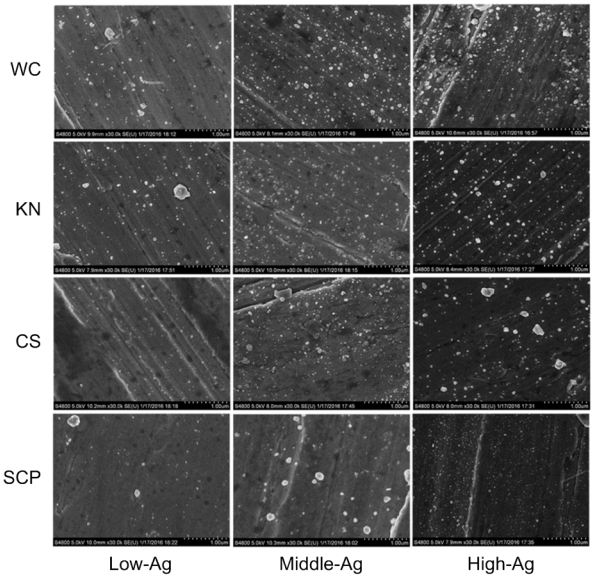

Fig. 2 SEM images of four dental castings (WC, KN, CS, and SCP) coated with silver nanoparticles of low, medium, and high concentrations

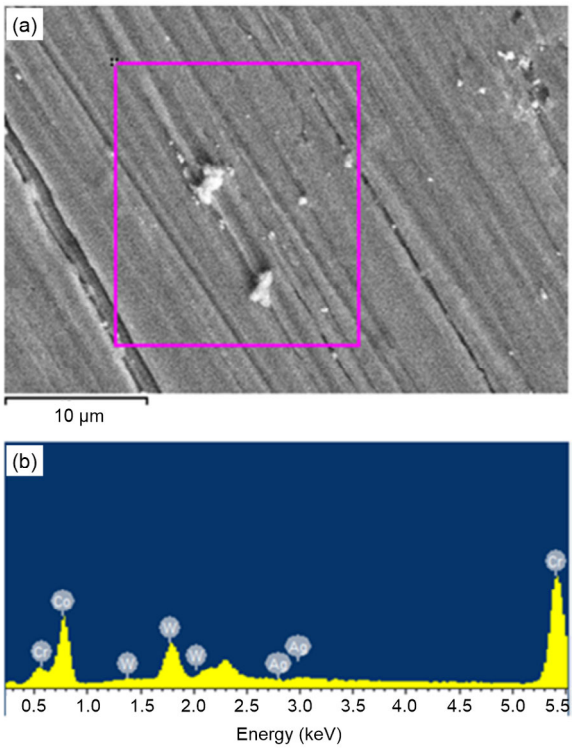

Fig. 3 SEM (a) and spectrum analysis (b) of KN coated with low concentration of silver nanoparticles

Table 1 Results of the spectrum analysis

Element	Molecular weight (%)	Atomic weight (%)
Cr	26.46	31.87
Co	59.35	63.07
Ag	0.94	0.55
W	13.25	4.51
Total	100.00	100.00

slightly greater amount at 5×10^4 and 5×10^5 cells/ml. The results were quite unexpected since cell seeding density had little effect on the general performances of the cells. The limited growing space of the petri dish in the monolayer culture may well explain the slight disadvantage at a lower density. However, at a higher density, the space of each model was only able to support a certain amount of cell growth and thus little relationship was observed between density and cell performances. From the two figures combined, 5×10^4 cells/ml was selected as the optimal cell seeding density when both indexes remained comparatively higher in the 3-D model.

After 2-d cultivation, the morphological appearance of the cylindroids was studied by histological analysis. Fig. 5a illustrates the overall morphology of the cylindroids, showing the relatively smooth and integrated surface of the cell aggregates. Under the same visual field, fluorescent image (Fig. 5b) was observed, indicating a compact and well-organized network of the cell cylindroids. The favorable growth conditions of the model were confirmed, with positive staining of cell nuclei throughout the entire cell aggregates. These images strongly suggest the success of the model in forming in vivo-like LO2 cylindroids.

In this section, we used very similar methods with the ones depicted by Chu et al. (2017). Yet with different types of cells lines (HepG2 cells in Chu et al. (2017) and LO2 cells in this study), we have the rationale to establish new conditions for further testing.

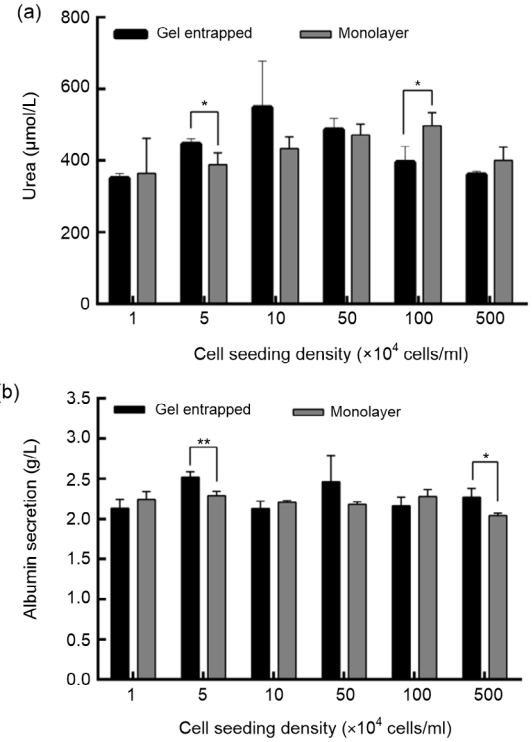

Fig. 4 Influence of different cell seeding densities on cell activity performance in the hollow fiber model and the monolayer model with graph in urea synthesis (a) and in albumin secretion (b)

* $P<0.05$, ** $P<0.01$, vs. the monolayer group. Data are expressed as mean±SD (n=3)

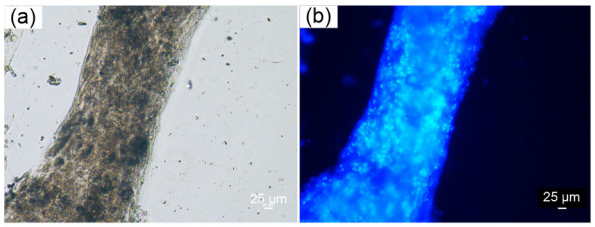

Fig. 5 Light image of the cylindroid (a) and fluorescence-stained image of the cylindroid (nuclei stained) (b) after 48 h culture

3.4 General evaluation of the model

After determining the seeding density, the culture medium in both models was sampled and refreshed every 2 d in the 10-d period for further metabolic tests. As shown in Fig. 6, during the 10-d cultivation period, both urea synthesis and albumin secretion in the 3-D model remained relatively high compared with the monolayer model, and these differences increased in the later period of culture, indicating significant differences in cellular activity after long-term cultivation.

The better performances of cells in the 3-D model can be well explained by the function of hollow fiber materials in material transportation, cell adhesiveness, and improvement of the functional expression of cells (Manivasagam et al., 2010). Also, the long-term maintenance of liver-specific functions in cylindroids has been proven possible by Mizumoto et al. (2008), suggesting up to 5-month maintenance of cylindrical morphology, ammonia removal, urea synthesis, and albumin secretion in certain culture media. Therefore, the model constructed was able to support the satisfactory growth of cell aggregates and ensure the stable functional expression of cells over a relatively long period.

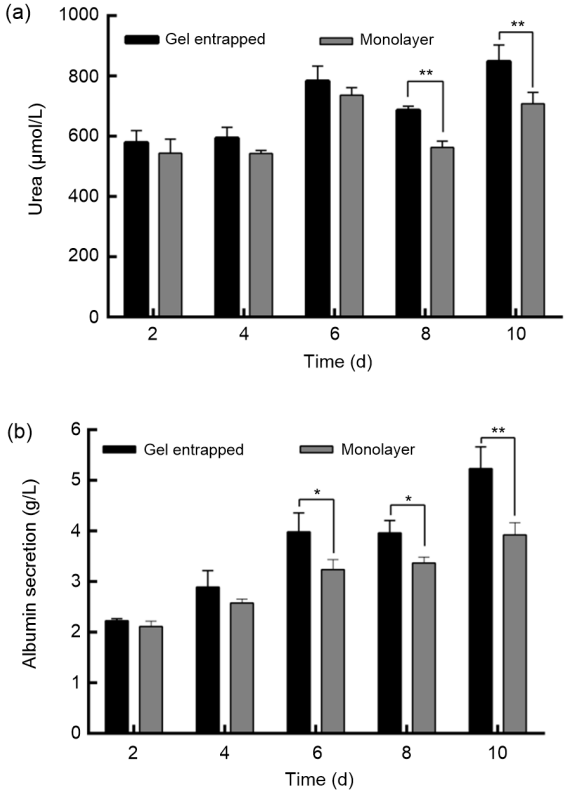

Fig. 6 Influence of culturing days on cell activity performance in the hollow fiber model and the monolayer model with graph in urea secretion (a) and in albumin secretion (b)

* $P<0.05$, ** $P<0.01$, vs. the monolayer group. Data are expressed as mean±SD (n=3)

3.5 Toxicity testing of the dental castings

Treated with the extract solution of the dental castings, Fig. 7 shows the results of MTT analysis in the form of cell viability where the values of the control groups (pure media without extract solution) were set as 100%. In Fig. 7a, after 24-h exposure, the 3-D model cells exposed to the extract of alloy WC and its variations showed an inverse relationship between cell deaths and the nanoparticle concentrations. Interestingly, unlike the positive correlations showed in former studies that had mainly focused on silver nanoparticles or coated nanoparticles alone (Silva et al., 2014), the results here indicate the benefits of using Ag nanoparticles as coating materials, as it mitigates the toxicity of pure castings. As shown in Fig. 7a, fewer cells suffered from the toxicity induced by the castings as the concentration of coated nanoparticles increased; this might be explained by the tightly wrapped nanoparticles preventing the release of alloy ions. Though slight improvements of toxicity due to the Ag nanoparticle coatings were demonstrated, the general toxicity of the castings was still aggravated with a longer exposure time since "aged" silver nanoparticles have been proven more toxic due to the slow dissolution of silver ions (Kittler et al., 2010) as well as the alloy itself. All other cultivated cells showed similar patterns to those treated with alloy WC's extract solution, with the coating of Ag nanoparticles mitigating the toxicity unexpectedly as their concentration increased, and a longer exposure time contributing to the toxicity of the castings due to the release of metal ions. Therefore, none of these processed Cr–Co castings are suitable for practical application based on the evaluation of their toxicity.

4 Conclusions

To test the toxicity of potential dental materials in an in vivo-like environment, we constructed a 3-D

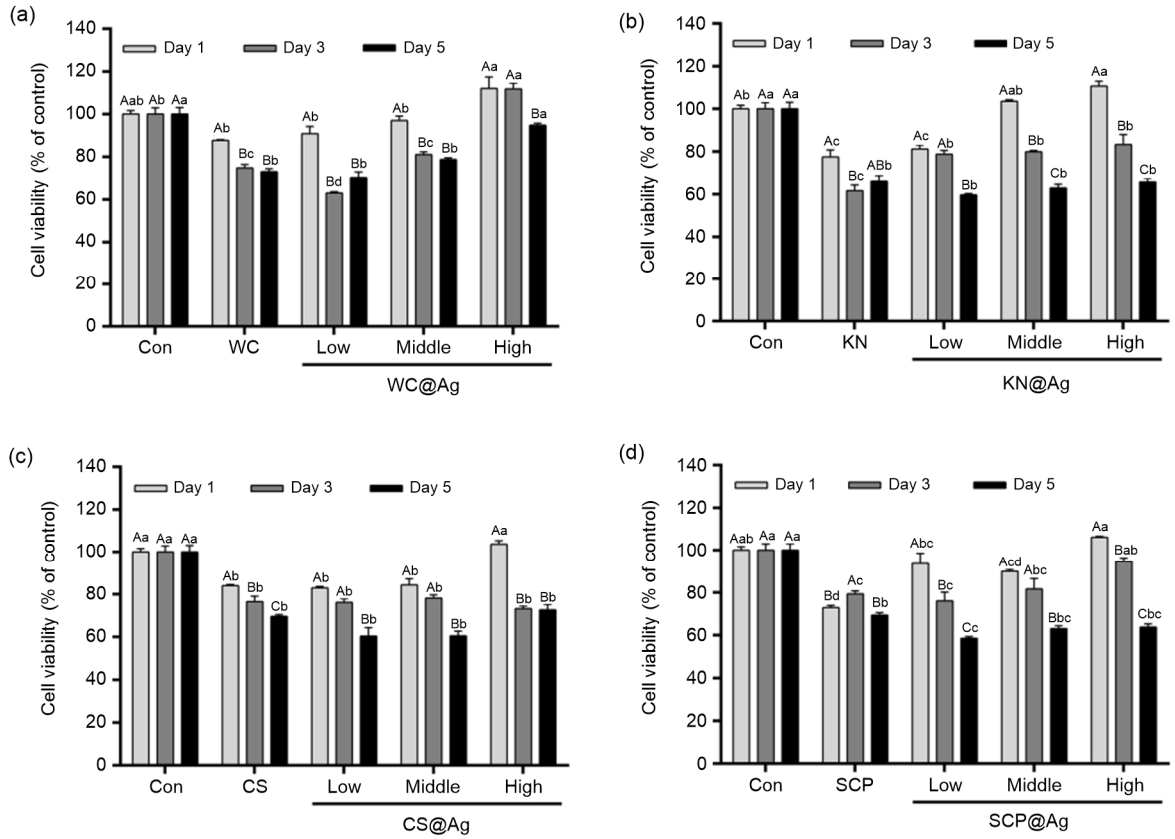

Fig. 7 Cell viability in the 3-D model after different exposure time (1, 3, and 5 d) to castings and castings with different concentrations of coated silver nanoparticles

(a) WC; (b) KN; (c) CS; (d) SCP. Data are expressed as mean±SD (n=3). $^{A–C}$ Different letters denote significant differences at the same concentrations of coated silver (P<0.05). $^{a–d}$ Different letters denote significant differences at the same exposure time (P<0.05)

cell model using PVDF membrane and the gel entrapment culture system. Compared with the traditional 2-D cell model, microscopic observations confirmed the 3-D morphology of the cell culture, while biochemical analysis identified the superiority of the model in regard of long-term maintenance and overall metabolic activity. Upon the successful model construction, we used MTT assays to briefly determine the toxicity of four types of silver nanoparticle-coated dental castings as a primary application. Through these series of experiments, we identified the mitigating effects of the silver nanoparticles on pure alloy toxicity and the time-induced aggravation of general toxicity in all types of castings regardless of coating, and thus proved the processed dental castings unsuitable for medical application based on the toxicity results on LO2 cells. The final toxicity may derive from the manufacturing process other than from the purchased alloys themselves. In general, the 3-D LO2 model constructed in this study provides a potential solution for the lack of accurate toxicity tests for silver nanoparticle-coated dental alloys in the field, and can be used to test other metallic biomedical materials in the future.

To clarify, our group also developed a 3-D model using HepG2 cells to test food-related chemical toxicities (Chu et al., 2017). However, in this model, we selected a more sensitive, normal cell line LO2 due to the moderate toxicity of dental castings. Additionally, the model constructed in this study is used to determine the toxicity of dental materials for the first time.

Compliance with ethics guidelines

Yi-ying ZHAO, Qiang CHU, Xu-er SHI, Xiao-dong ZHENG, Xiao-ting SHEN, and Yan-zhen ZHANG declare that they have no conflict of interest.

This article does not contain any studies with human or animal subjects performed by any of the authors.

References

Al-Hiyasat AS, Bashabsheh OM, Darmani H, 2002. Elements released from dental casting alloys and their cytotoxic effects. *Int J Prosthodont*, 15(5):473-478.

Aksakal B, Yildirim OS, Gul H, 2004. Metallurgical failure analysis of various implant materials used in orthopedic applications. *J Fail Anal Prev*, 4(3):17-23. https://doi.org/10.1007/s11668-996-0007-9

Allaker RP, 2010. The use of nanoparticles to control oral biofilm formation. *J Dent Res*, 89(11):1175-1186. https://doi.org/10.1177/0022034510377794

AshaRani PV, Mun GLK, Hande MP, et al., 2009. Cytotoxicity and genotoxicity of silver nanoparticles in human cells. *ACS Nano*, 3(2):279-290. https://doi.org/10.1021/nn800596w

Burcham PC, 2014. Target-organ toxicity: liver and kidney. In: An Introduction to Toxicology. Springer London, p.151-187. https://doi.org/10.1007/978-1-4471-5553-9_6

Chu Q, Zhao Y, Shi X, et al., 2017. In vivo-like 3-D model for sodium nitrite- and acrylamide-induced hepatotoxicity tests utilizing HepG2 cells entrapped in micro-hollow fibers. *Sci Rep*, 7(1):14837. https://doi.org/10.1038/s41598-017-13147-z

Dambach DM, Andrews BA, Moulin F, 2005. New technologies and screening strategies for hepatotoxicity: use of in vitro models. *Toxicol Pathol*, 33(1):17-26. https://doi.org/10.1080/01926230590522284

de Bartolo L, Salerno S, Morelli S, et al., 2006. Long-term maintenance of human hepatocytes in oxygen-permeable membrane bioreactor. *Biomaterials*, 27(27):4794-4803. https://doi.org/10.1016/j.biomaterials.2006.05.015

Fadeel B, Garcia-Bennett AE, 2010. Better safe than sorry: understanding the toxicological properties of inorganic nanoparticles manufactured for biomedical applications. *Adv Drug Deliv Rev*, 62(3):362-374. https://doi.org/10.1016/j.addr.2009.11.008

García-Contreras R, Argueta-Figueroa L, Mejía-Rubalcava C, et al., 2011. Perspectives for the use of silver nanoparticles in dental practice. *Int Dent J*, 61(6):297-301. https://doi.org/10.1111/j.1875-595X.2011.00072.x

Gómez-Lechón MJ, Castell JV, Donato MT, 2007. Hepatocytes—the choice to investigate drug metabolism and toxicity in man: *in vitro* variability as a reflection of *in vivo*. *Chem Biol Interact*, 168(1):30-50. https://doi.org/10.1016/j.cbi.2006.10.013

Hamouda IM, 2012. Current perspectives of nanoparticles in medical and dental biomaterials. *J Biomed Res*, 26(3): 143-151.

Hanawa T, 2002. Evaluation techniques of metallic biomaterials in vitro. *Sci Technol Adv Mater*, 3(4):289-295. https://doi.org/10.1016/S1468-6996(02)00028-1

Hiromoto S, Noda K, Hanawa T, 2002. Development of electrolytic cell with cell-culture for metallic biomaterials. *Corros Sci*, 44(5):955-965. https://doi.org/10.1016/S0010-938X(01)00110-X

Hussain SM, Hess KL, Gearhart JM, et al., 2005. In vitro toxicity of nanoparticles in BRL 3A rat liver cells. *Toxicol in Vitro*, 19(7):975-983. https://doi.org/10.1016/j.tiv.2005.06.034

Kino Y, Sawa M, Kasai S, et al., 1998. Multiporous cellulose microcarrier for the development of a hybrid artificial liver using isolated hepatocytes. *J Surg Res*, 79(1):71-76. https://doi.org/10.1006/jsre.1998.5389

Kittler S, Greulich C, Diendorf J, et al., 2010. Toxicity of silver nanoparticles increases during storage because of slow dissolution under release of silver ions. *Chem Mater*, 22(16):4548-4554. https://doi.org/10.1021/cm100023p

Kmieć Z, 2001. Cooperation of liver cells in the synthesis and degradation of eicosanoids. In: Cooperation of Liver Cells in Health and Disease. Springer Berlin Heidelberg, p.51-59.

Li Y, Lv XL, 2001. Research progress of modification of poly (vinylidene fluoride) porous membrane. *J Tianjin Polytech Univ*, 5:74-78.

Manivasagam G, Dhinasekaran D, Rajamanickam A, 2010. Biomedical implants: corrosion and its prevention—a review. *Recent Pat Corros Sci*, 2(1):40-54. https://doi.org/10.2174/1877610801002010040

Mizumoto H, Ishihara K, Nakazawa K, et al., 2008. A new culture technique for hepatocyte organoid formation and long-term maintenance of liver-specific functions. *Tissue Eng Part C Methods*, 14(2):167-175. https://doi.org/10.1089/ten.tec.2007.0373

Morones JR, Elechiguerra JL, Camacho A, et al., 2005. The bactericidal effect of silver nanoparticles. *Nanotechnology*, 16(10):2346-2353. https://doi.org/10.1088/0957-4484/16/10/059

Niinomi M, Hattori T, Morikawa K, et al., 2002. Development of low rigidity β-type titanium alloy for biomedical applications. *Mater Trans*, 43(12):2970-2977. https://doi.org/10.2320/matertrans.43.2970

Ren YB, Yang C, Liang Y, 2002. Research and development of new biomedical metallic material. *Mater Rev*, 16(2): 12-15.

Schmalz G, Langer H, Schweikl H, 1998. Cytotoxicity of dental alloy extracts and corresponding metal salt solutions. *J Dent Res*, 77(10):1772-1778. https://doi.org/10.1177/00220345980770100401

Silva T, Pokhrel LR, Dubey B, et al., 2014. Particle size, surface charge and concentration dependent ecotoxicity of three organo-coated silver nanoparticles: comparison between general linear model-predicted and observed toxicity. *Sci Total Environ*, 468-469:968-976. https://doi.org/10.1016/j.scitotenv.2013.09.006

Sung JH, Ji JH, Yoon JU, et al., 2008. Lung function changes in Sprague-Dawley rats after prolonged inhalation exposure to silver nanoparticles. *Inhal Toxicol*, 20(6):567-574. https://doi.org/10.1080/08958370701874671

Wataha JC, 2000. Biocompatibility of dental casting alloys: a review. *J Prosth Dent*, 83(2):223-234. https://doi.org/10.1016/S0022-3913(00)80016-5

Wong KKY, Cheung SOF, Huang L, et al., 2009. Further evidence of the anti-inflammatory effects of silver nanoparticles. *Chem Med Chem*, 4(7):1129-1135. https://doi.org/10.1002/cmdc.200900049

Yamamoto A, Honma R, Sumita M, 1998. Cytotoxicity evaluation of 43 metal salts using murine fibroblasts and osteoblastic cells. *J Biomed Mater Res*, 39(2):331-340. https://doi.org/10.1002/(SICI)1097-4636(199802)39:2<331::AID-JBM22>3.0.CO;2-E

Zreiqat H, Howlett CR, Zannettino A, et al., 2002. Mechanisms of magnesium-stimulated adhesion of osteoblastic cells to commonly used orthopaedic implants. *J Biomed Mater Res*, 62(2):175-184. https://doi.org/10.1002/jbm.10270

中文概要

题　目：LO2 细胞 3-D 模型用于四种纳米银包裹的牙科合金材料毒性的检测

目　的：应用体外三维模型模拟肝脏组织微环境，更真实地反映和评估纳米银材料和牙科合金对于人体的潜在毒性。

创新点：借助中空纤维管和胶原蛋白首次构建了 LO2 细胞三维聚集体，并将该模型应用到医用材料毒性的评价中。

方　法：首先，采用扫描电镜观察中空纤维材料的孔径，确保营养物质的正常交换。然后，将混合有胶原蛋白的细胞悬液注入到中空纤维管的内胆，通过尿素氮和白蛋白检测，确定最佳细胞密度进行长期培养。在显微镜下观察细胞聚集体的形态，确保模型的成功建立。其次，应用水热法制作纳米银颗粒并将颗粒包裹到预先购买的合金材料上。最后，用不同牙科材料的浸提液培养细胞 1、3 和 5 天，通过 MTT 检测细胞死亡率，从而间接评价材料的毒性。

结　论：中空纤维材料的表征结果显示该材料具有较好的耐热性和细胞粘附性，孔径大小适宜营养物质交换，可以应用到三维模型的构建中。通过白蛋白和尿素氮两个指标来评价三维模型的活性，发现每毫升 5×10^4 细胞的浓度最适宜细胞生长（图 4）。进一步模型评价表明，相比于传统单层培养的细胞，三维模型中的细胞能保持长期活力（图 6）且可以在更短时间内对低药物浓度作出反应。

关键词：LO2细胞；三维模型；纳米银；牙科合金；毒性检测